Article

Pharmacological Evaluation of Cannabinoid Receptor Modulators Using GRAB$_{\text{eCB2.0}}$ Sensor

Samay Shivshankar [1], Josephine Nimely [1], Henry Puhl III [2] and Malliga R. Iyer [1,*]

1 Section on Medicinal Chemistry, National Institute on Alcohol Abuse and Alcoholism, National Institutes of Health, 5625 Fishers Lane, Rockville, MD 20852, USA
2 Laboratory of Biophotonics and Quantum Biology, National Institute on Alcohol Abuse and Alcoholism, National Institutes of Health, 5625 Fishers Lane, Rockville, MD 20852, USA; puhlh@mail.nih.gov
* Correspondence: malliga.iyer@nih.gov

Abstract: Cannabinoid receptors CB_1R and CB_2R are G-protein coupled receptors acted upon by endocannabinoids (eCBs), namely 2-arachidonoylglycerol (2-AG) and *N*-arachidonoyl ethanolamine (AEA), with unique pharmacology and modulate disparate physiological processes. A genetically encoded GPCR activation-based sensor that was developed recently—GRAB$_{\text{eCB2.0}}$—has been shown to be capable of monitoring real-time changes in eCB levels in cultured cells and preclinical models. However, its responsiveness to exogenous synthetic cannabinoid agents, particularly antagonists and allosteric modulators, has not been extensively characterized. This current study expands upon the pharmacological characteristics of GRAB$_{\text{eCB2.0}}$ to enhance the understanding of fluorescent signal alterations in response to various functionally indiscriminate cannabinoid ligands. The results from this study could enhance the utility of the GRAB$_{\text{eCB2.0}}$ sensor for in vitro as well as in vivo studies of cannabinoid action and may aid in the development of novel ligands.

Keywords: GRABeCB2.0; 2-AG; CB1R; CB2R; AEA; allosteric; orthosteric

1. Introduction

The endocannabinoid system (ECS) is a sophisticated mechanism comprising signaling pathways and endogenous modulators that intricately regulate various processes in the human body [1]. Specifically, endocannabinoids (eCBs) such as 2-arachidonoylglycerol (2-AG) and *N*-arachidonoyl ethanolamine (AEA), interact with the G-protein coupled cannabinoid receptors CB_1 and CB_2, activating them in distinct ways and influencing various signaling processes uniquely [2,3]. Notably, these same receptors recognize the active component of marijuana, Δ^9-tetrahydrocannabinol (THC). Both CB_1 and CB_2 receptors play a crucial role in various physiological and pathophysiological processes in the central nervous system and peripheral tissues [4]. CB_1 receptors are prominently expressed in the brain, where they are one of the most highly expressed GPCRs, and at lesser yet significantly operative levels in peripheral tissues like the lung, liver, and kidney [5]. CB_2 receptors, on the other hand, are mainly found in immune cells as well as hematopoietic systems, although brain CB_2 receptors have also been extensively documented [5–7].

The primary intracellular regulators activated by CB_1R are heterotrimeric G proteins from the $G_{(i/o)}$ family. The G-protein subunits inhibit adenylyl cyclase while also modulating ion channels, including those for calcium and potassium ions [8]. Activation of CB_1R additionally results in the phosphorylation and activation of mitogen-activated protein kinases (MAPK), such as p42/p44 MAPK, p38 MAPK, and c-Jun N-terminal kinase, which have the capacity to regulate nuclear transcription factors [8]. Furthermore, activated and phosphorylated CB_1R form associations with β-arrestin, leading to complexes which can contribute to receptor desensitization and internalization [9]. The expansive reach of CB_1R across the human body and the multitude of physiological pathways in which it participates make it a strong candidate for pharmaceutical targeting [10].

The endocannabinoid/CB_1R system (ECS) is a crucial regulator of lipid and carbohydrate metabolism [11,12]. CB_1R activation promotes energy conservation and inhibits energy expenditure, with an overactive ECS contributing to the development of visceral obesity and the associated metabolic syndrome [13–15]. CB_1R antagonists show promising anti-obesity effects and cardiometabolic improvements in obese subjects, yet the clinical utility of the receptor has not been harnessed beyond the now-withdrawn agent Acomplia (rimonabant) due to unacceptable neuropsychiatric side effects [16,17]. Hence, tools and probes advancing the understanding of the CB_1R-based pathway hold great promise to develop safer therapeutics based on this mechanism of action (MoA) [15,18,19].

To monitor real-time fluctuations in eCB lipid mediator levels in cultured cells and rodent models acting through CB_1R, an elegant tool in the form of a genetically encoded fluorescent sensor named $GRAB_{eCB2.0}$ has been developed [20]. Its activation by eCB analogs produced by cells and limited phytocannabinoids has also now been characterized [21]. This characterization is crucial for enhancing the tool's effectiveness in studying the pharmacological actions of cannabinoids in vivo. However, many CB_1R ligands and would-be therapeutics are exogenous, lipophilic, synthetic ligands belonging to numerous different chemotypes whose ability to interact with $GRAB_{eCB2.0}$ is still unclear. Understanding the interaction and binding dynamics of these probes could offer additional utility for $GRAB_{eCB2.0}$ and opportunities to improve the sensor technology broadly for in vitro and in vivo pharmacological application [22–24]. In the current study we sought to analyze the actions of various classes of synthetic cannabinoid ligands on the $GRAB_{eCB2.0}$ sensor. The results obtained here present a window into utilizing the CB_1R-based $GRAB_{eCB2.0}$ for the rapid assessment of apparent binding affinities and preliminary functional characterization of tested ligands. While the sensor is predominantly activated by compounds that act on the receptor as agonists, we have now developed a robust method for measuring apparent binding affinities of compounds that do not inherently activate the sensor but behave as CB_1 functional antagonists/inverse agonists.

As a standard GPCR, the effects of eCBs and pharmaceutical ligands for drug discovery are measured using many standardized assays on CB_1Rs. These assays include radioligand binding, GTPγS, cAMP, β-arrestin, BRET-based assays, and many more [25]. These assays work to discover binding affinities and the activity of the receptor in the presence of different modulators. These assays can, at times, pose challenges when dealing with radioisotopes, sophisticated instruments, and convoluted protocols, along with prohibitively expensive assay reagents. Li and co-workers have developed the novel $GRAB_{eCB2.0}$ sensor, engineered from CB_1R, by incorporating a circularly permutated-green fluorescent protein (cpGFP) in intracellular loop 3 (ICL3), where the native receptor interacts with heterotrimeric G-proteins [20]. Through iterative approaches, the sensor was shown to be a fast, reliable, cell-based tool that can qualitatively divulge activity and apparent binding of eCBs and modulators of the CB_1R. This sensor works via the conformational change caused in the transmembrane domain when a modulator binds and causes the fluorescence of GFP to change. This sensor lacks the functional signaling domains of the receptor and allows for measurement through the visualization of the increased fluorescence upon binding to the sensor by way of activation. As developed, the sensor has been shown to exhibit robust fluorescence increases when exposed to the eCBs AEA and 2-AG in cultured neural cells, acute brain tissue slices, and targeted brain tissues in vivo, such as the amygdala and hippocampus. In cultured HEK293 cells, live cell confocal microscopy and fluorescent signal measurements were used to test many eCBs, phytocannabinoids, and prototypical CB_1R antagonist SR141617A (rimonabant) by Stella and coworkers [21].

The $GRAB_{eCB2.0}$ sensor has been proven to help detect eCBs and exogenous ligands. As an extension, in the current study, we validate the sensor's performance to detect synthetic agonists and now show that the sensor-based measurements allow for an expedient assay that can uncover antagonist potencies of CB_1R modulators based on its ability to displace agonists. We also tested known and reported allosteric modulators, both positive and negative, for effects on the sensor. Branching this method towards novel compounds

will allow one to conduct a fast, reliable assay that can ascertain qualitatively whether a modulator behaves as an agonist or antagonist.

2. Results and Discussion

2.1. $GRAB_{eCB2.0}$ Assays for CB1R Agonists

Agonists of the CB_1 receptor have been shown to have therapeutic effects in various animal models and clinical trials [18]. CB1 receptor agonists work as an antinociceptive to combat acute and chronic pain, reduce symptoms of stress and anxiety, and elevate symptoms of withdrawal in chronic drug-dependent patients for long-term alcohol, cannabis, and opiate use [26]. Yet, psychotropic properties limit the clinical use of many cannabinoid agonists [27]. The $GRAB_{eCB2.0}$ sensor was initially designed to look at ligand dynamics of endocannabinoids that are part of the ECS and thus, upon ligand binding, show concentration-dependent increase in fluorescence. Validating previous work, we show that synthetic, exogenous agonists as well as components of the ECS like 2-AG and AEA respond to the sensor as reported [20,21] (see Figure 1A,B, Section 3).
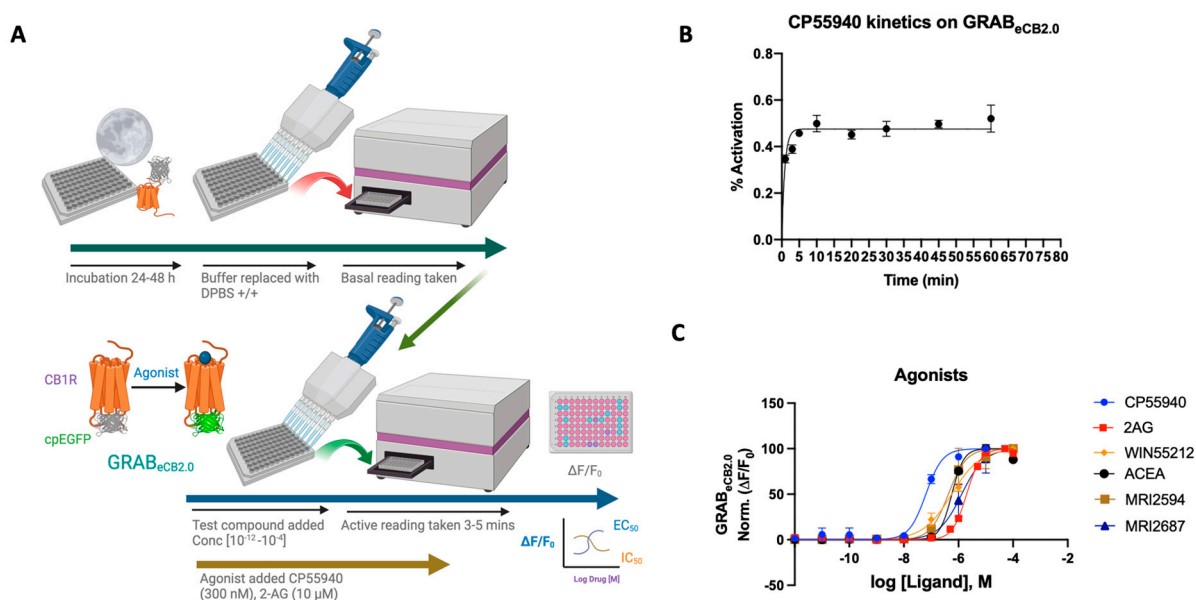

Figure 1. (**A**) Schematic depiction of the assay principle of the reported $GRAB_{eCB2.0}$ sensor optimized in HEKtsA201 cells. Agonist binding activates the sensor, inducing a change in fluorescence. (**B**) Kinetics graph of 300 nM CP55940 run at varying incubation time periods of 1, 3, 5, 10, 20, 30, 45, and 60 min. Plateau occurs after 5 min with limited deviation from the normal. Optimum time points for reading between 4 and 7 min. (**C**) Concentration-dependent responses and EC_{50}s of 2-AG, ACEA, CP55940, WIN55212-2, MRI-2594, and MRI-2687 at inducing $GRAB_{eCB2.0}$ fluorescent signal, as determined by averaging $\Delta F/F_0$ normalized between 4 and 5 min (*vide infra*). EC_{50} values were calculated by GraphPad Prism 9. Data represent mean $\pm$ SEM from minimum three independent experiments.

2-AG is a naturally occurring endocannabinoid with a relatively high concentration in the central nervous system [28]. Using the $GRAB_{eCB2.0}$ sensor in HEK293 cells, an EC_{50} of ~2 µM was obtained for 2-AG, showing an increase in fluorescence upon ligand binding. This is in line with reported data using the $GRAB_{eCB2.0}$ sensor, delivering an EC_{50} for 2-AG at a value of 3.1 µM [20]. The reported EC_{50} of 2-AG by Stella's group was 85 nM [21] (Figure 1C).

CP-55,940 is a strong CB_1 receptor full agonist with a reported binding affinity 45 times that of Δ^9-tetrahydrocannabinol (THC), the active compound found in marijuana [29,30]. CP-55,940 has also been published to have therapeutic effects as both an antinociceptive and an antiemetic [31]. However, reported adverse effects of CP-55,940 preclude its use as a therapeutic [32]. As a potent CB_1 receptor agonist, the reported EC_{50} of CP-55,940 ranges

from the sub-nanomolar value of 0.04 nM to 31 nM. The $GRAB_{eCB2.0}$ sensor under our reported conditions delivered an apparent EC_{50} of 64 ± 8 nM.

WIN55212-2 is a potent full agonist of the CB_1 receptor and has been used in experimental as well as clinical studies [33–36]. Mice treated with WIN55212-2 have been shown to have a significant reduction in pain, making it a plausible analgesic [37]. Clinical studies using WIN55212-2 have shown that the modulator can reduce interocular pressure in patients with glaucoma resistant to other therapies [34]. Reportedly, WIN55212-2 has an EC_{50} ranging from 5.5 nM to 3000 nM [37]. Using the sensor in HEK cells, an EC_{50} of 564 ± 34 nM was achieved in the range of reported values. As tested previously, the plot displays a strong agonist curve, giving both qualitative and quantitative validity and reported for EC_{50} [20].

ACEA is a CB_1 selective agonist that shares much of its chemical structure with AEA, an endocannabinoid produced in the central nervous system. ACEA has been shown to bind (Ki = 1.5–5 nM) with a reported EC_{50} of 51 nM for the CB_1 receptor [38]. It has also been used for its therapeutic effects on the ECS as an antidepressant and nociceptive, and it works as an anticonvulsant in patients with epilepsy [38]. ACEA on the $GRAB_{eCB2.0}$ sensor functions as an agonist, but with a diminished EC_{50} of 572 ± 4 nM. We also assayed CB_2R agonist/antagonist pair MRI-2594 and MRI-2687 to test their CB_1 binding activity via their ability to modulate the sensor fluorescence [39]. As reported, the compounds indeed show weak CB_1 agonism upon sensor binding, where EC_{50} = 527 ± 27 nM and 1.3 μM, respectively.

In all cases tested, the agonists activated the sensor, increased the fluorescence and valid EC_{50}s could be obtained. It should be noted that the agonists for $GRAB_{eCB2.0}$ expressed in HEK293 cells activated the sensor differentially, possibly indicating differing ligand dynamics. Altogether the sensor offers a viable tool that can be activated concentration-dependently and used to determine the EC_{50} of the ligand upon binding to the sensor, the EC_{50} values obtained in general varied to a significant extent (at least 10×) in comparison to the literature-reported values obtained using wild-type CB_1R or membrane preparation.

2.2. $GRAB_{eCB2.0}$ Assays for Antagonist/Inverse Agonists

Antagonists of the CB_1R have been sought for their potential beneficial effects in obesity, metabolic disorders, fibrosis, and drug dependence [15,40]. Previous work with the sensor has shown both rimonabant and AM251 decrease sensor fluorescence [20]. Stella and coworkers reported that rimonabant, decreased $GRAB_{eCB2.0}$ signal responses with a reported IC_{50} value of 3.3 nM, mirroring its reported potency for CB_1R [21]. We sought to investigate the responses of various CB_1 antagonists belonging to differing chemotypes on the $GRAB_{eCB2.0}$ sensor. Prototypical CB_1 antagonists are classified as 3-arm bearing compounds. CB_1 antagonists like rimonabant, taranabant, and otenabant belong to the 3-arm class based on their orientation in the inactive binding of CB_1 in the crystal structure [41].

2.3. 3-Arm Modulators

With a standardized procedure in hand, we validated rimonabant's behavior on the GRAB sensor. The literature-reported potencies for rimonabant range from an IC_{50} of 5.6 nM to 48 nM [42]. The treatment of rimonabant on the $GRAB_{eCB2.0}$ sensor stable HEK293 cells showed an inhibition of fluorescence and below baseline level indicative of inverse agonism (measured EC_{50} = 42 ± 3 nM, Figure 2A). This is in line with reported data for rimonabant by Stella and co-workers. However, in mimicking the antagonist functional assay, the sensor could be activated by agonists like CP559450 or 2-AG. The CP559450 quench by an antagonist could be concentration-dependently observed by decreased fluorescence showing antagonism and producing a potent CB_1 antagonist curve for rimonabant in the same experimental system. An area of concern was the lipophilicity of the ligands tested in the assay. The HEK293 cells are kept viable in the 96-well plate with DPBS buffer. The DPBS buffer poses challenges in dissolving highly lipophilic cannabinoid agents. To combat this

problem, optimum inclusion of bovine serum albumin (BSA) was tested and 0.5 mg/mL BSA was implemented in the buffer to increase the solubility of ligands (Supplementary Materials, Figure S1). In principle, this approach could be exploited to derive the apparent 'inactivating' binding IC_{50} values for the antagonist ligands in the presence of an agonist. Thus, we assayed the effects of ligands altering sensor dynamics in the absence and in the presence of BSA.
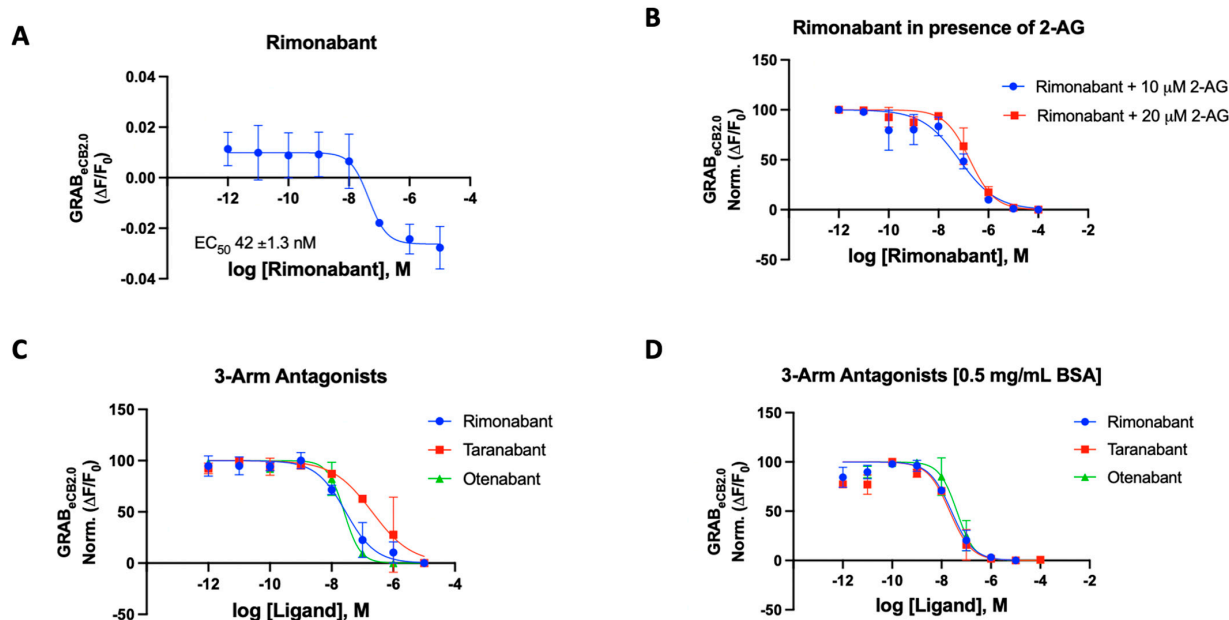

Figure 2. (**A**) Fluorescent signal of rimonabant at inhibiting $GRAB_{eCB2.0}$ basal fluorescence as determined by averaging $\Delta F/F_0$ between 4 and 5 min. (**B**) Antagonist potency of rimonabant at inhibiting $GRAB_{eCB2.0}$ fluorescence in presence of 10 mM and 20 mM of 2-AG, as determined by averaging $\Delta F/F_0$ normalized between 4 and 5 min. (**C**) Antagonist potency of 3-arm ligands at inhibiting $GRAB_{eCB2.0}$ fluorescence in presence of 300 nM of CP55940 and in absence of BSA, as determined by averaging $\Delta F/F_0$ normalized between 4 and 5 min. (**D**) Antagonist potency of 3-arm ligands at inhibiting $GRAB_{eCB2.0}$ fluorescence in presence of 300 nM of CP55940 with 0.5 mg/mL BSA, as determined by averaging $\Delta F/F_0$ normalized between 4 and 5 min. IC_{50} values were calculated by GraphPad Prism 9. Data represent mean $\pm$ SEM from minimum three independent experiments (Table 1).

Table 1. Effect of 3-arm antagonists in modulating $GRAB_{eCB2.0}$ fluorescence in presence of 300 nM CP55940.

Compound	$GRAB_{eCB2.0}$ IC_{50} [nM]	$GRAB_{eCB2.0}$ IC_{50} [nM] 0.5 mg/mL BSA
Rimonabant	31 ± 9.5	25 ± 2.5
Taranabant	205 ± 15	23 ± 5
Otenabant	27 ± 7.5	41 ± 4.8

For rimonabant, we tested the sensor in the various modes using 2-AG (10 and 20 µM) and CP55940 (300 nM) as the activating ligand in the presence and absence of BSA (Figure 2B–D) [43]. In our 96-well plate reader assay using the HEK293 cells, the potency of rimonabant on the $GRAB_{eCB2.0}$ was largely not affected by the presence of BSA in the buffer. The IC_{50} values were remarkably consistent for rimonabant using various experimental agonists with and without BSA (Figure 2B–D). In the presence of 300 nM CP55940, rimonabant suppressed the increase in fluorescence caused by CP55940 on $GRAB_{eCB2.0}$ modified CB_1 receptors, resulting in a calculated IC_{50} of 31 nM reflecting

its antagonist potency. It can be stated that, for this compound, there is valid qualitative and quantitative data proving the fidelity of this sensor. Rimonabant was also tested to antagonize 2-AG, a weaker agonist in comparison to CP55940. Agonist concentrations of 10 μM 2-AG gave IC_{50} of 56 ± 2.3 nM and with 20 μM of 2-AG, an IC_{50} of 181 ± 52 nM was obtained for rimonabant. We then proceeded to test the various known and literature-reported antagonists of cannabinoid CB_1 receptor. Qualitative data could be derived for all compounds to determine if the modulator is an antagonist, corresponding to its ability to affect the basal fluorescence as well as in the presence of an agonist. In the presence of a constant concentration of CP55940 (300 nM), known antagonists were added to the cells, leading to an observed suppression of fluorescence emitted by the modified CB_1Rs. These assays were conducted on a concentration gradient, with the modulator's concentration ranging from 10^{-12} to 10^{-5} for each compound.

Taranabant, another potent inverse agonist/antagonist for the CB_1R, produced an IC_{50} value of 205 nM on the $GRAB_{eCB2.0}$. This reported Ki of taranabant is 0.13 nM and it showed robust effects in antagonizing CP55940 actuated fluorescence [41,44]. Otenabant is another highly potent antagonist for the CB_1R that was in clinical trials [45,46]. Similar to taranabant, otenabant was under development as an anti-obesity agent, but clinical trials were halted when rimonabant's malaise-inducing effects came into light. Otenabant has a reported IC_{50} of 13.1 nM with a binding Ki of 0.7 nM for CB_1R [46]. The $GRAB_{eCB2.0}$ sensor gave a qualitative curve showing the antagonistic effects of the compound in the assay, also giving an IC_{50} of 27 nM in the presence of 300 nM CP55940.

The $GRAB_{eCB2.0}$ sensor showed robust antagonist responses for prototypical CB_1 antagonists, with taranabant being an exception. Thus, the sensor can be used with novel compounds when testing for the effect the synthesized modulators on the CB_1 receptor. Upon addition of BSA, the IC_{50}s of the compounds improved for taranabant but surprisingly not for rimonabant and otenabant (Table 1). Taranabant improved to 23 nM IC_{50} in response to the BSA inclusion in the buffer compared to the original 205 nM IC_{50}. An IC_{50} value of 41 nM was obtained for otenabant upon the addition of BSA.

2.4. 4-Arm Modulators

New class of compounds developed in the last decade which function through peripheral mechanisms like JD5037 and, more recently, Zevaquenabant (MRI-1867), Monlunabant (MRI-1891), and MRI-1776. A defining structural feature of these novel compounds is that they belong to the 4-arm antagonist class. In contrast to the previously tested 3-arm antagonist, they contain an additional branch or "arm" arising from the central carbon (Figure 3A). This additional arm can potentially offer unique interactions with certain amino acids in the inactive CB_1R binding pocket [47–53]. Our laboratory has been developing such novel, 4-arm, peripherally-restricted antagonists of the CB_1R, which have shown promise in ameliorating fibrosis of the liver, lung, skin, kidney and treating dyslipidemia, insulin resistance, obesity and attenuating alcohol drinking in rodent models [50–57]. A recent Phase 1b study in patients with metabolic syndrome has shown that MRI-1891/INV-202/Monlunabant causes a significant decrease in body weight and improvement in cardiometabolic parameters without any adverse effects [58]. The 4-arm antagonist developed in our lab provided us an opportunity to test their behavior on the $GRAB_{eCB2.0}$ sensor and their ability to antagonize agonist responses.
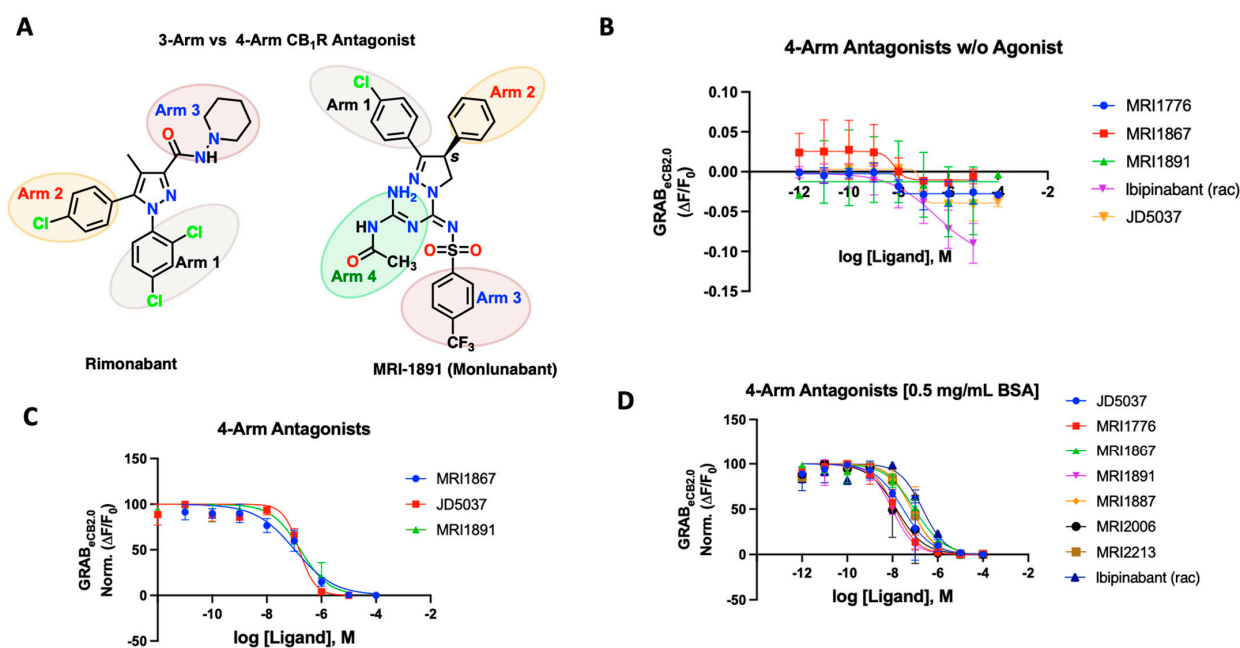
Figure 3. (**A**) Structural depiction of prototypical 3-arm and 4-arm CB_1R antagonists. (**B**) Fluorescent signal of 4-arm modulators ibipinabant, JD5037, MRI-1867, MRI-1891, and MRI-1776 at inhibiting $GRAB_{eCB2.0}$ basal fluorescence, as determined by averaging $\Delta F/F_0$ between 4 and 5 min. (**C**) Antagonist potency of select 4-arm ligands JD5037, MRI-1867, and MRI-1891 at inhibiting $GRAB_{eCB2.0}$ fluorescence in presence of 300 nM of CP55940 and in absence of BSA, as determined by averaging $\Delta F/F_0$ normalized between 4 and 5 min. (**D**) Antagonist potency of select 4-arm modulators ibipinabant, JD5037, MRI-1776, MRI-1867, MRI-1891 MRI-1887, MRI-2213, and MRI-2006 (all compounds tested were enantiomerically pure (*S*)-isomer) at inhibiting $GRAB_{eCB2.0}$ fluorescence in presence of 300 nM of CP55940 with 0.5 mg/mL BSA, as determined by averaging $\Delta F/F_0$ normalized between 4 and 5 min. IC_{50} values were calculated by GraphPad Prism 9. Data represent mean ± SEM from minimum three independent experiments (*vide infra*, Table 2).

Table 2. Antagonism IC_{50} values of prototypical 4-arm modulators on $GRAB_{eCB2.0}$ in the absence of BSA and in the presence of 0.5 mg/mL BSA.

Compound	$GRAB_{eCB2.0}$ IC_{50} [nM]	$GRAB_{eCB2.0}$ IC_{50} [nM] 0.5 mg/mL BSA
MRI-1867	105 ± 5.4	90 ± 5
MRI-1891	168 ± 57	9.8 ± 1.4
JD5037	148 ± 12	29 ± 3.5

We tested various compounds for putative interaction of the fourth arm with the receptor residues and its dynamics upon binding to the receptor. Prototypical compounds JD5037, MRI-1891/Monlunabant, and MRI-1867/Zevaquenabant were tested for their ability to alter sensor dynamics in the presence and absence of CP55940 (Figure 3B–D). JD5037, discovered by Chorvat and colleagues, is a peripherally-restricted analog of the CB_1R antagonist compound ibipinabant (SLV319) [59]. Ibipinabant has a truncated fourth arm which, upon modification, led to the compound JD5037 via an extended fourth arm conferred by a valinamide moiety that led to a potent antagonism on the CB_1R with binding Ki = 0.5 nM [59,60]. On the $GRAB_{eCB2.0}$ sensor, the 4-arm antagonists inhibited the fluorescence of the sensor, leading to a concentration-dependent alteration below the baseline, indicative of inverse agonism (Figure 3B). We also tested the antagonists to inhibit agonist fluorescence in the presence of CP55940 (300 nM). JD5037 delivered an IC_{50} of 148 nM, much lower than that of the reported value. MRI-1867 is another

reported CB_1R antagonist with a functional potency IC_{50} of 40 nM and binding Ki of 2.6 nM; the GRAB-based sensor gave a much lower IC_{50} of 105 nM. MRI-1891 is also a potent 4-arm CB_1R antagonist with a bias toward inhibition of the β-arrestin pathway, over G-protein signaling pathway (IC_{50} = 6 nM) and binding Ki = 0.5 nM. When applied to the $GRAB_{eCB2.0}$, MRI-1891 yielded an IC_{50} of 168 nM. Of note, the 4-arm modulators clearly revealed their ability to reverse the increase in CP55940-mediated fluorescence and behave as antagonists, highlighting the utility of the $GRAB_{eCB2.0}$ to differentiate the functional character of the test compounds (Figure 3C). As previously seen, all tested 4-arm antagonists benefited significantly from the addition of the BSA in the buffer (Figure 3D). MRI-1867 improved to 90 nM, MRI-1891's IC_{50} on the sensor improved to 9.8 nM, and finally JD5037 improved to 29 nM in the presence of the same agonist-concentration (Table 2). The sensor enabled us to derive apparent potencies of additional 4-arm antagonists that were previously reported, as reflected in Figure 3D (Table S1, Supplementary Materials). In general, the binding potencies trended toward the lower range on the sensor, in comparison to the reported affinities using the wild-type CB_1R or membrane preparation and were comparable to the functional potencies reported for the compounds. The tested compounds were mainly enantiomerically pure *S*-isomers which were reported earlier to have single-digit nanomolar binding affinities (Table S1, Supplementary Materials) [47,49–53]. The CB_1 active enantiomer (*S*)- and (*R*)- enantiomer (inactive) could be clearly distinguished on the sensor. For example, the *R*-enantiomers of MRI-1891 and MRI-1776 were reported to have weak CB1 binding and upon testing on the sensor, this was clearly the case (Supplementary Materials, Figure S2).

2.5. $GRAB_{eCB2.0}$ Assays for Allosteric Modulators

Allosteric modulation is considered one pathway to alter CB_1R signaling, while minimizing deleterious side effects associated with direct orthosteric interaction [61,62]. To broaden the pharmacological characterization of $GRAB_{eCB2.0}$ using the 96-well plate reader assay, we sought to investigate the dynamics of the literature-reported allosteric compounds on the sensor [63–65]. Stella and colleagues reported the characteristics of cannabidiol (CBD), which acts as a CB_1R negative allosteric modulator (NAM) on the sensor [21]. It was found that increasing concentrations of CBD did not affect basal $GRAB_{eCB2.0}$ fluorescent signal. We sought to investigate various reported synthetic allosteric compounds like ORG27569 (ORG), PSNCBAM-1 (PSN) and pregnenolone analogues for their behavior on the sensor [65]. ORG27569 has been characterized as an allosteric modulator that shows positive cooperativity for CP55940 binding to CB_1 but paradoxically acts as an antagonist of G-protein coupling [66,67]. PSNCBAM-1 was characterized as a NAM based on detailed pharmacological assays, but it enhances agonist binding [68]. Pregnenolone (Preg) is classified as a signaling specific negative allosteric modulator on the CB_1R [64]. When applied to the $GRAB_{eCB2.0}$, while the compounds ORG27569 and Preg did not significantly alter basal fluorescence, PSN showed weak inverse agonism at higher concentrations (Figure 4A). Upon checking their behavior on the sensor in the presence of 300 nM CP55940, all three compounds extinguished the CP-activation differentially; however, their behavior was void of any concentration-dependent effects, in contrast to antagonists like rimonabant (Figure 4B). For PSN and Preg, this behavior could be replicated in the presence of 20 μM 2-AG (Supplementary Materials, Figure S3A–C). In the presence of 300 nM CP55940, a normalized curve of ORG and PSN indicated their behavior as weak antagonists with IC_{50} 787 nM and 567 nM (Supplementary Materials, Figure S3B). Pregnenolone sulfate was also checked for allosteric effects in presence of CP. $GRAB_{eCB2.0}$sensor behavior showed that this compound also extinguished CP fluorescence but showed no concentration-dependent effects (Supplementary Materials, Figure S3D).

Using the optimized assay in a traditional orthosteric manner works well and delivers reliable agonist and antagonist potencies. The sensor was then tested for its ability to determine the difference between competitive and non-competitive antagonism in an assay mirroring the Schild regression analysis [68,69]. Rimonabant's robust results as an

orthosteric antagonist made it a good competitor with minimum variance in the solubility and potency of its effect. To test for the ability to detect competitive binding on the sensor at the orthosteric position, rimonabant and PSNCBAM-1 (individually) were added on the 96-well plate in a Schild-plot manner, as described in Section 3. Despite the lack of signaling attributes in the sensor, the GRAB$_{eCB2.0}$ sensor could derive the receptor's activity based on fluorescence in the same mechanistic manner as a traditional assay would and could relay the same regression analysis with strong quantitative correlations. We tested rimonabant in an 'apparent' Schild plot using varying concentrations of CP55940 against select concentrations of rimonabant (Figure 4C). Rimonabant, a competitive inverse agonist, resulted in a concentration-dependent increase in the EC$_{50}$ of CP55940. The Schild plot for rimonabant provided a gradient/slope of 1.1, indicating competitive reversible antagonism of an orthosteric nature (Figure 4C).
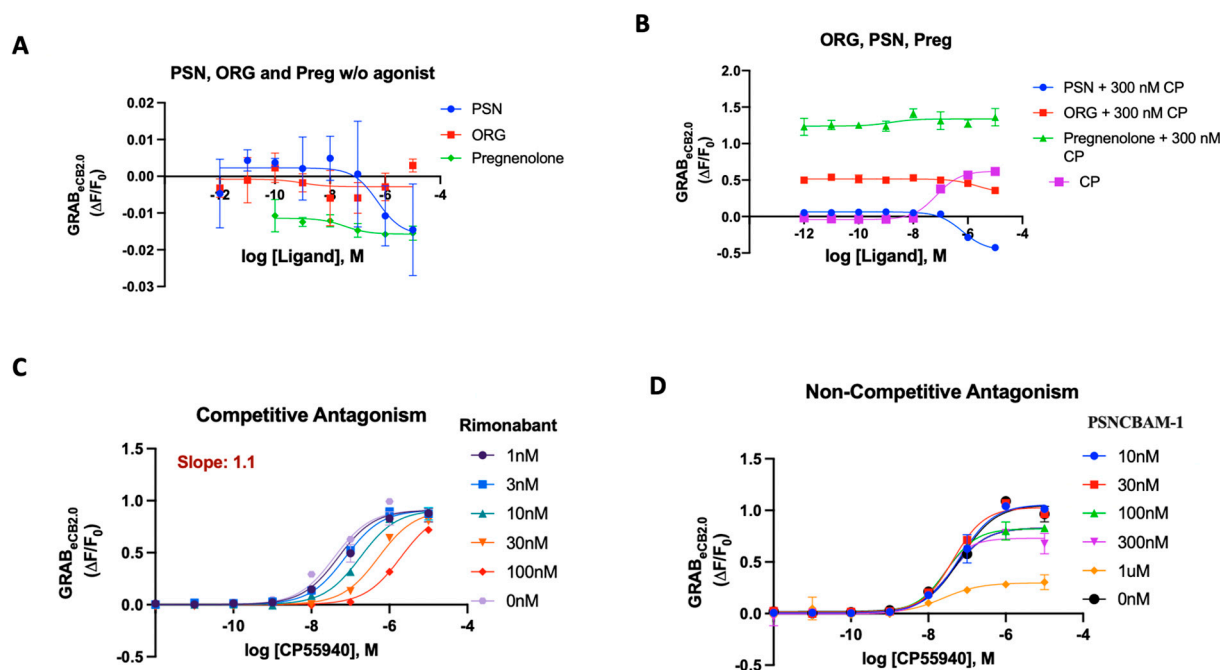

Figure 4. (**A**) Fluorescent signal of ORG, PSN and Pregnenolone at inhibiting GRAB$_{eCB2.0}$ basal fluorescence as determined by averaging $\Delta F/F_0$ between 4 and 5 min. (**B**) Antagonist potency of ORG PSN and Pregnenolone at inhibiting GRAB$_{eCB2.0}$ fluorescence in presence of 300 nM of CP55940; CP activation of the sensor for reference as determined by averaging $\Delta F/F_0$ between 4 and 5 min. (**C**) Competitive antagonism of rimonabant in the presence of a range of concentrations of CP55940. Curves were fitted to a nonlinear regression model with four parameters, variable for individual concentrations. Data for rimonabant were used to generate a Schild plot. On application of the Gaddum–Schild equation, a gradient/slope of 1.13 was obtained. (**D**) In presence of a range of concentrations of CP55940, differing from rimonabant, PSN did not significantly affect the EC$_{50}$ value of CP55940. However, the fluorescent response of CP55940 was reduced in a concentration-dependent manner, indicating non-competitive antagonism. EC$_{50}$/IC$_{50}$ values were calculated by GraphPad Prism 9. Data represent mean of minimum three independent experiments.

Through detailed [^{35}S]-GTPγS and cAMP assays, PSN was characterized as a non-competitive antagonist using a Schild regression analysis [68]. When PSN was tested in our assay with varying concentrations of CP55940, as described above, the eCB2.0 sensor displayed a behavior that pointed to its non-competitive attributes (Figure 4D). Unlike a competitive antagonist, PSN did not significantly affect the EC$_{50}$ value of CP55,940. However, the efficacy/fluorescent response (apparent equivalent of E_{max}) of CP55,940 was reduced in a concentration-dependent manner. These data provide validation that PSNCBAM-1 can behave as a non-competitive antagonist on the GRAB$_{eCB2.0}$ sensor.

We also tested the literature-reported positive allosteric modulators (PAMs) of CB_1R for their ability to influence the sensor. Commercially available compounds GAT228 and GAT229, which are chiral and enantiomers of racemic GAT211 and are both well characterized, were procured. In various biological systems examined, GAT211's allosteric agonist activity was shown to reside with the *R*-(+)-enantiomer (GAT228), whereas the *S*-(-)-enantiomer (GAT229), which showed no intrinsic activity, is where the PAM activity resided [70].

In the case of the $GRAB_{eCB2.0}$ sensor, both GAT modulators were initially used independently to see if there would be any alteration in the fluorescence signal. Both compounds delivered a weak enhancement of the signal, demonstrating activity as a very weak agonist (EC_{50} 2 and 1 μM, respectively) (Figure 5A). When compared to CP55940, both GAT compounds showed a very weak increase in fluorescence (Supplementary Materials, Figure S4). As previously reported, we then proceeded to test both GAT228 and GAT 229's ability to interact with the sensor in the presence of CP55940 (300 nM). As shown in Figure 5B, GAT229 was a more potent enhancer of sensor fluorescence than GAT228. This result seemingly agrees with the report that GAT229 does positively modulate the agonist response/fluorescence. GAT228, then, behaves as an allosteric agonist, by virtue of its weak agonism. Upon testing both compounds in Schild-like analyses (Figure 5C,D) to evaluate the positive allosteric effect, we could discern the difference in the characteristics of the curve by their α values. GAT228 had apparent α remaining constant at all concentrations of the agonist, whereas GAT229 had an apparent $\alpha > 1$. This result aligns with the reported behavior of GAT228 and GAT229, although the sensor does not unambiguously discern the difference in the allosteric subtilities expected with these ligands. An additional detail of the differential effects of the compounds GAT228 and GAT229 could be seen when GAT228 (1 μM) did not shift the fluorescence signal relative to orthosteric ligand CP55940, whereas GAT229 (1 μM) increased the maximal fluorescence induced by CP55,940 in the sensor experimental system.

$GRAB_{eCB2.0}$ was recently designed and reported by Li and colleagues to allow for the detection of change in fluorescent signal in response to changes in endocannabinoid levels in the ECS. Our interest in this sensor was piqued when we envisioned that it could be used as a tool to assay novel cannabinoid modulators. In a simple assay that could potentially offer a 'hybrid binding-function' evaluation tool for novel ligands, we sought to develop a method to test functionally indiscriminate CB_1R modulators. As such, we optimized the sensor system/assay to generate EC_{50s} for compounds that increase the fluorescence with existing agonists so they could be validated on the sensor, as previously reported. For modulators that do not increase the basal fluorescence, we could determine the functional characteristics of the ligands by the compound's ability to suppress an agonist-induced fluorescence increase in an assay supporting traditional functional assays like $[^{35}S]$-GTPγS or cAMP. The sensor also performed reasonably well to detect previously reported allosteric compounds. Allosteric binding sites on GPCRs are discrete domains in the 7-transmembrane or intracellular regions distinct from orthosteric sites that bind ligands causing a potentiation or attenuation of orthosteric ligand mediated effects and result from changes in protein conformation. Extensive studies have illuminated the NAM effects of PSN ligand. Accordingly, we tested PSN in cell culture in the absence and presence of CP55940. PSN, in the absence of CP, showed no increase above basal fluorescence, while allosteric effects could be detected upon a Schild-like analysis. GAT228 and GAT229, in the presence of 300 nM CP55940, showed allosteric effects mirroring their reported behavior [70]. At the sensor, a distinguishing characteristic of the orthosteric antagonists vs. the allosteric antagonists was the clear concentration-dependent attenuation of agonist fluorescence that was absent in allosteric compounds. In principle, this agrees with the fact that allosteric compounds can affect orthosteric ligand binding from sites far away from the traditional putative binding pocket, and their responses vary based on the ligand in use. This is an area that will require additional evaluation and optimization of the assay

parameters to study and validate novel allosteric modulators; the sensor construct devoid of signaling components may limit the study of intricate allosteric mechanisms involved.
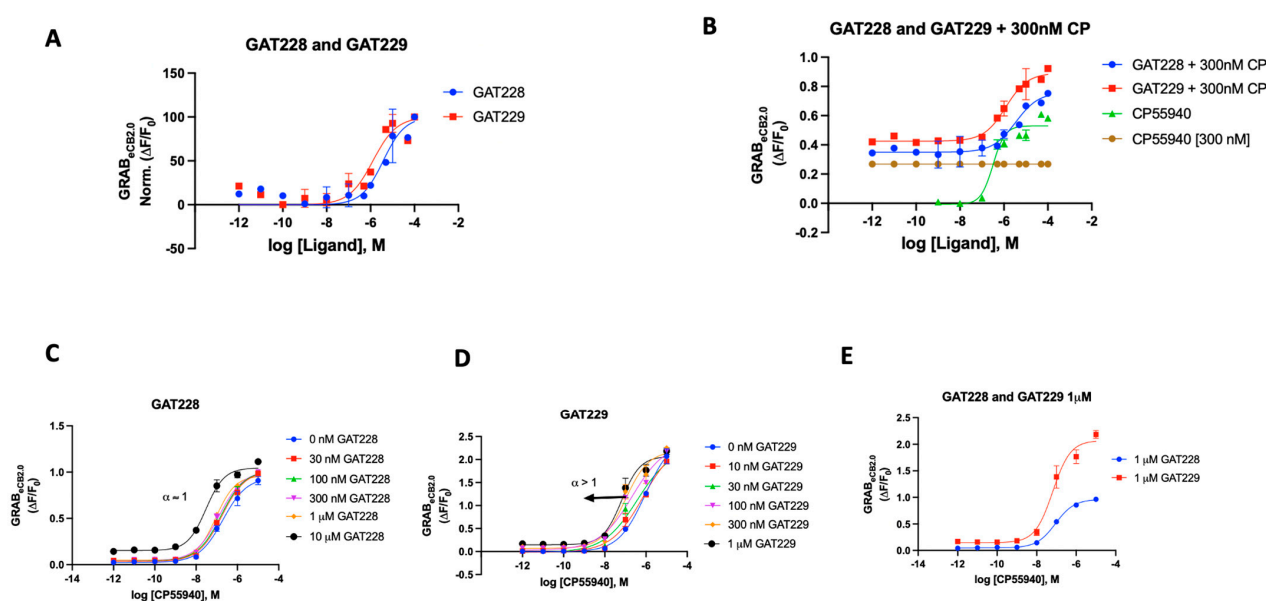

Figure 5. (**A**) Fluorescent signal of GAT228 and GAT229 at altering $GRAB_{eCB2.0}$ basal fluorescence as determined by averaging $\Delta F/F_0$ normalized between 4 and 5 min. (**B**) Fluorescent signal of GAT228 and GAT229 at altering $GRAB_{eCB2.0}$ fluorescence in presence of 300 nM CP55940, as determined by averaging $\Delta F/F_0$ between 4 and 5 min. (**C**) Non-competitive agonism of GAT228 in the presence of a range of concentrations of CP55940. Curves were fitted to a nonlinear regression model with four parameters, variable for individual concentrations. (**D**) Non-competitive agonism of GAT228 in the presence of a range of concentrations of CP55940. (**E**) Fluorescent signal of GAT228 and GAT229 (1 μM), altering $GRAB_{eCB2.0}$ fluorescence in presence of varying concentrations of CP55940, as determined by averaging $\Delta F/F_0$ between 4–5 min. Curves were fitted to a nonlinear regression model with four parameters, with variable slope. EC_{50} values were calculated by GraphPad Prism 9. Data represent mean of minimum three independent experiments.

As discussed before, the CB_1 modulators are highly lipophilic compounds which may pose challenges with solubility to dissolve readily in the aqueous buffer. This does seem to influence IC_{50} values, which initially were lower than reported. BSA dissolved in the DPBS aqueous buffer at a concentration of 0.5 mg/mL, increasing the solubility of the lipophilic modulators and resulting in increased congruence to reported EC_{50}/IC_{50} values for many of the modulators. Of note, the agonist ligands were tested for their ability to affect the sensor signal in the presence of BSA. This resulted in a larger variance from the reported EC_{50} values (Supplementary Materials, Figure S5).

An additional factor that can alter the sensor performance for certain compounds is the amino acid mutations in the sensor construct. This was particularly evident in cases of the antagonists containing a fourth arm. The binding affinity of the fourth arm with the mutated amino acids plays a role in this differentiation and the hydrophobicity of the molecule itself. 2-AG and rimonabant-like 3-arm antagonists are purported to interact with certain amino acids within the orthosteric binding site in CB1R that are likely present in $GRAB_{eCB2.0}$. The optimized $GRAB_{eCB2.0}$ sensor has a serine-to-threonine mutation at the 383rd residue (S383T) and a phenylalanine-to-alanine mutation at the 177th position (F177A). These mutations were induced in the sensor CB_1R to increase the fluorescence of the attached GFP and allow for better detection. The fourth arm in compounds MRI-1891 and MRI- 1776 were proposed to have interaction with amino acid residues S383 and F177 [49,51–53]. Mutated amino acids in the sensor region that are not present in native CB_1R may contribute to subtle change in binding dynamics and hence, varied IC_{50}s could

be seen for such compounds using this sensor. The steric features of the arm and the functional groups may further play a role in the interaction and the activity of the receptors in such modulators.

3. Materials and Methods

Chemicals and Reagents: 2-AG (Cayman, Ann Arbor, MI, USA #62160), CP55940 (Cayman #13608), ACEA (Biotechne, Minneapolis, MN, USA: Tocris #1319), SR141716 (MedChem Express, New York, NY, USA: #HY14136), Taranabant (MedChem Express #HY10013), Otenabant (MedChem Express #HY-10871), Ibipinabant (MedChem Express HY-14791), and GAT228 and GAT229 (MilliporeSigma: Burlington, MA, USA #SML1952 and #SML1951). ORG27569 (Tocris #2957), PSNCBAM-1 (Cayman #25855), Pregnenolone and Pregnenolone sulfate (Thermo Fisher, Waltham, MA, USA: #AC164420050 and # 537650), JD5037, MRI-1867, MRI-1891, MRI-1776, MRI-1887, MRI-2213, MRI-2594, MRI-2687, and MRI-2006 (structures of compounds in Supplementary Materials, Table S1) were synthesized in-house according to previously published procedures [49–53,59,60].

Stable eCB2.0 sensor cell line: A stable sensor cell line was established in HEKtsA201 cells (Sigma-Aldrich, St. Louis, MO, USA) using the PiggyBac Transposon-based system (SBI, Palo Alto, CA, USA). Briefly, the open reading frame of the eCB2.0 sensor from eCB2.0 to C1[20] was cloned into the PB514B shuttle vector using In Fusion cloning (Takara, San Jose, CA, USA). The modified shuttle sequence was obtained with Sanger sequencing (Psomagen, Rockville, MD, USA) and verified (MacVector, Apex, NC, USA). HEKtsA201 cells were maintained in DMEM (Thermo Fisher, Waltham, MA, USA: Gibco #10569-010) supplemented with 10% fetal bovine serum (Gibco #A31605-01) and 1% penicillin/streptomycin (Gibco #15140-122) at 37 °C and 8% CO_2. Cells were plated on 12-well tissue culture plates at approximately 50% confluency. This low cell density was used to avoid overgrowth of the cells during the delay between transfection and selection for stable integration. After 3 h, the eCB2.0 shuttle was co-transfected at a plasmid mass ratio of 10:1 with the SBI Transposase vector (PB210PA) using deacylated PEI [71]. All transfected wells were checked the next day for expression of the sensor by presence of basal cpeGFP fluorescence. Sensor expression produced weak eGFP signal as expected; however, the PB514B shuttle carries an RFP (Red Fluorescent Protein) open reading frame driven off a separate Puromycin resistance expression cassette. Hence RFP reporter expression was also monitored. Wells were selected for integration beginning at 4 days post transfection with 10 mg/mL Puromycin (Gibco #A11138-03). Selection was continued throughout all passages of the stable line. Cells were transferred to T25 (25 cm^2) tissue culture flasks after 10 to 14 days of selection.

Assay Procedure: The DMEM solution was removed from the T25 flat-sided cell culture flask by decantation. A total of 3 mL of TrypLE (Gibco #12604-021) was added and allowed to incubate for 2–3 min at 25 °C in a laminar flow hood. A total of 7 mL of fresh DMEM was added, and cells were gently pipetted to remove any remaining cells from the flask wall. The total volume (10 mL) was transferred to a 15 mL Falcon tube and centrifuged at $800 \times g$ for 4 min at 23 °C. Upon completion of centrifugation, the supernatant was removed and discarded, leaving behind a small pellet of cells that were resuspended in 4 mL of fresh DMEM. The cell suspension was mixed in a 1:1 ratio with 0.4% TrypanBlue (10 mL each) and 10 mL of the combined solution was added to each side of a Countess Cell Counting Chamber and inserted into the Countess II Automated Cell Counter (Thermo Fisher, Waltham, MA, USA). The concentration of cells as adjusted to 0.7–1.0 million cells/mL with DMEM complete media and 100 mL was added to the desired wells of a clear bottom black plastic tissue culture treated 96-well plate. The plate was incubated at 37 °C and 8% CO_2 for a 24–48 h period. After incubation, the 100 mL DMEM buffer was removed and replaced with 100 mL of DPBS buffer containing calcium and magnesium (Gibco #14040-133). After the addition of the DPBS buffer, a baseline reading of the cells was taken using the PHERAstar FSX microplate reader (BMG/Labtech, Cary, NC, USA) to establish the F0 or initial fluorescence (see Figure 1A,B).

When running the assay for an agonist, 25 mL of the compound and 25 mL of additional DPBS buffer was added to the wells. A concentration curve was made for the modulator with the final concentrations in the wells holding the cells ranging from 1 pM to 10 mM with 1% DMSO BSA in a total volume of 150 mL. The procedure was reapplied to check for EC_{50} values upon inclusion of 0.5 mg/mL BSA in the buffer. The procedure was modified for compounds that did not show an increase in fluorescence upon testing (presumed antagonist/allosteric modulators). A total of 25 μL of the compound and 25 μL of additional DPBS buffer or 25 μL of a standardized agonist (CP55940 or 2-AG) were used to assess fluorescence alterations in the presence and absence of an agonist. A concentration curve was made for the modulator with the final concentration in the wells holding the cells ranging from 1 pM to 10 μM, and the final concentration of the CP55940 in the well was 300 nM (10 or 20 μM if 2-AG) with 1% DMSO and 0.5 mg/mL BSA in a total volume of 150 μL. In either assay, the cannabinoid ligands were added, followed by incubation of the compound on the cells at 37 °C for 5 min before taking a fluorescence reading using the PHERAstar FSX microplate reader equipped with a GFP filter cube module (Ex. 485 nm/Em. 520 nm). The recorded values were the F or final fluorescence.

For reported allosteric modulators, the binding assay was modified to test the ligand for basal activity, followed by the addition of the agonist, similar to the antagonist assay. To assess competitive or non-competitive antagonism, the sensor was tested in an assay akin to the Schild analysis [69,72,73]. The concentration of CP55940 varied from concentrations of 1 pM to 10 mM. The compound of interest was varied across concentrations ranging (as the case may be) from 1 nM, 3 nM, 10 nM, 30 nM, 100 nM, 300 nM, 1 μM, and 10 μM and performed in triplicate. The concentration of the compound depended on the modulator itself. The concentrations calculated were the final concentration inside the well of the 96-well plate, along with the 1% DMSO and 0.5 mg/mL BSA (See Supplementary Materials, Figure S1). A 5 min incubation time was sufficient for detection of peak assay activity as any earlier time points had not reached maximum intensity, and all time points after 5 min show a sustained plateau (See Figure 1B).

Statistical Methods: All $GRAB_{eCB2.0}$ fluorescent signals (in cases noted) are expressed as normalized $\Delta F/F_0$ as calculated for the fluorescence assay in the PHERAstar FSX Plate reader. EC_{50}/IC_{50} values were calculated using GraphPad Prism 9 by fitting data to a nonlinear regression model with normalized variable slope (four parameters, normalized where indicated) or using three-parameter response. Data represent mean ± SEM from a minimum of at least three independent experiments performed in triplicates.

4. Conclusions

In an approach amenable to a high-throughput or 96-well plate reader assay platform in HEK293 cells, we show that 2-AG, CP55940, WIN5512, ACEA, MRI-2594, and MRI-2687 increase the $GRAB_{eCB2.0}$ fluorescent signal and behave as agonists of CB_1R. However, the extent of the increase in fluorescence differs with EC_{50} values that are modestly comparable to wildtype CB1R estimated radioligand binding. Expanding on the utility of the $GRAB_{eCB2.0}$, we also observed that rimonabant dose-dependently blocks the agonist mediated increase in the $GRAB_{eCB2.0}$ fluorescent signal, with an IC_{50} in line with its reported potency at CB_1R. In the absence of an agonist, rimonabant's effect modulating the sensor could be measured at levels below baseline fluorescent signal, suggesting inverse agonism. This effect was indeed seen for other tested antagonists, including 4-arm ligands. Various antagonists were validated with the sensor for their ability to antagonize the agonist-induced fluorescence increase, supporting the use of $GRAB_{eCB2.0}$ as a pharmacological tool. PSN modulated the CP-induced increase in the $GRAB_{eCB2.0}$ fluorescent signal but not its basal fluorescent signal significantly. In a method mimicking Schild analysis, PSN's behavior indicated that the non-competitive molecular mechanism seen in native CB_1R is maintained in $GRAB_{eCB2.0}$. In similar experiments, rimonabant unambiguously behaved as a competitive, orthosteric antagonist. Indeed, rimonabant behaved as a tool compound with high fidelity on the sensor, further attesting to its utility as a control for sensor-based experiments in the current

model system. Allosteric behavior using PAMs were also gleaned on the sensor. Thus, GRAB$_{eCB2.0}$ provides an opportunity to study changes in the binding dynamics of NAMs, PAMs and functionally disparate CB$_1$ ligands belonging to varied chemotypes in a robust in vitro cell culture system. Our results delineate and validate the pharmacological profiles and binding dynamics of cannabinoid receptor ligands using a GRAB$_{eCB2.0}$ sensor system and offer opportunities for improving the sensor technology to 'sense' subtle changes induced by ligands with privileged and yet-to be explored chemotypes targeting the endocannabinoid CB$_1$ receptor in a simple model platform. Further validation of the sensor should be possible through future studies on novel ligands with varying cannabinoid receptor functional profiles.

References

1. Rodríguez de Fonseca, F.; Del Arco, I.; Bermudez-Silva, F.J.; Bilbao, A.; Cippitelli, A.; Navarro, M. The endocannabinoid system: Physiology and pharmacology. *Alcohol Alcohol.* **2005**, *40*, 2–14. [CrossRef] [PubMed]
2. Howlett, A.C.; Abood, M.E. CB1 and CB2 receptor pharmacology. *Adv. Pharmacol.* **2017**, *80*, 169–206. [PubMed]
3. Howlett, A.C.; Barth, F.; Bonner, T.I.; Cabral, G.; Casellas, P.; Devane, W.A.; Felder, C.C.; Herkenham, M.; Mackie, K.; Martin, B.R.; et al. International Union of Pharmacology. XXVII. Classification of cannabinoid receptors. *Pharmacol. Rev.* **2002**, *54*, 161–202. [CrossRef]
4. Pacher, P.; Bátkai, S.; Kunos, G. The Endocannabinoid System as an Emerging Target of Pharmacotherapy. *Pharmacol. Rev.* **2006**, *58*, 389–462. [CrossRef]
5. Galiegue, S.; Mary, S.; Marchand, J.; Dussossoy, D.; Carriere, D.; Carayon, P.; Bouaboula, M.; Shire, D.; Le Fur, G.; Casellas, P. Expression of Central and Peripheral Cannabinoid Receptors in Human Immune Tissues and Leukocyte Subpopulations. *Eur. J. Biochem.* **1995**, *232*, 54–61. [CrossRef]
6. Onaivi, E.S.; Ishiguro, H.; Gong, J.P.; Patel, S.; Perchuk, A.; Meozzi, P.A.; Myers, L.; Mora, Z.; Tagliaferro, P.; Gardner, E.; et al. Discovery of the Presence and Functional Expression of Cannabinoid CB2 Receptors in Brain. *Ann. N. Y. Acad. Sci.* **2006**, *1074*, 514–536. [CrossRef]
7. Cabral, G.A.; Raborn, E.S.; Griffin, L.; Dennis, J.; Marciano-Cabral, F. CB2 receptors in the brain: Role in central immune function. *Br. J. Pharmacol.* **2008**, *153*, 240–251. [CrossRef] [PubMed]
8. Turu, G.; Hunyady, L. Signal transduction of the CB1 cannabinoid receptor. *J. Mol. Endocrinol.* **2009**, *44*, 75–85. [CrossRef]
9. Delgado-Peraza, F.; Ahn, K.H.; Nogueras-Ortiz, C.; Mungrue, I.N.; Mackie, K.; Kendall, D.A.; Yudowski, G.A. Mechanisms of Biased β-Arrestin-Mediated Signaling Downstream from the Cannabinoid 1 Receptor. *Mol. Pharmacol.* **2016**, *89*, 618–629. [CrossRef]
10. Pacher, P.; Kunos, G. Modulating the endocannabinoid system in human health and disease—Successes and failures. *FEBS J.* **2013**, *280*, 1918–1943. [CrossRef]

11. Sun, L.-J.; Yu, J.-W.; Wan, L.; Zhang, X.-Y.; Shi, Y.-G.; Chen, M.-Y. Endocannabinoid system activation contributes to glucose metabolism disorders of hepatocytes and promotes hepatitis C virus replication. *Int. J. Infect. Dis.* **2014**, *23*, 75–81. [CrossRef] [PubMed]

12. Gatta-Cherifi, B.; Cota, D. New insights on the role of the endocannabinoid system in the regulation of energy balance. *Int. J. Obes.* **2016**, *40*, 210–219. [CrossRef] [PubMed]

13. Han, J.H.; Kim, W. Peripheral CB1R as a modulator of metabolic inflammation. *FASEB J.* **2021**, *35*, e21232. [CrossRef] [PubMed]

14. Rajesh, M.; Bátkai, S.; Kechrid, M.; Mukhopadhyay, P.; Lee, W.-S.; Horváth, B.; Holovac, E.; Cinar, R.; Liaudet, L.; Mackie, K.; et al. Cannabinoid 1 receptor promotes cardiac dysfunction, oxidative stress, inflammation, and fibrosis in diabetic cardiomyopathy. *Diabetes* **2012**, *61*, 716–727. [CrossRef] [PubMed]

15. Cinar, R.; Iyer, M.R.; Kunos, G. The therapeutic potential of second and third generation CB1R antagonists. *Pharmacol. Ther.* **2020**, *208*, 107477. [CrossRef] [PubMed]

16. Janero, D.R.; Makriyannis, A. Cannabinoid receptor antagonists: Pharmacological opportunities, clinical experience, and translational prognosis. *Expert Opin. Emerg. Drugs* **2009**, *14*, 43–65. [CrossRef] [PubMed]

17. Ward, S.J.; Raffa, R.B. Rimonabant Redux and Strategies to Improve the Future Outlook of CB1 Receptor Neutral-Antagonist/Inverse-Agonist Therapies. *Obesity* **2011**, *19*, 1325–1334. [CrossRef] [PubMed]

18. Pertwee, R.G. Cannabinoid receptor ligands: Clinical and neuropharmacological considerations, relevant to future drug discovery and development. *Expert Opin. Investig. Drugs* **2000**, *9*, 1553–1571. [CrossRef] [PubMed]

19. Sharma, M.K.; Murumkar, P.R.; Kanhed, A.M.; Giridhar, R.; Yadav, M.R. Prospective therapeutic agents for obesity: Molecular modification approaches of centrally and peripherally acting selective cannabinoid 1 receptor antagonists. *Eur. J. Med. Chem.* **2014**, *79*, 298–339. [CrossRef]

20. Dong, A.; He, K.; Dudok, B.; Farrell, J.S.; Guan, W.; Liput, D.J.; Puhl, H.L.; Cai, R.; Wang, H.; Duan, J.; et al. A fluorescent sensor for spatiotemporally resolved imaging of endocannabinoid dynamics in vivo. *Nat. Biotechnol.* **2022**, *40*, 787–798. [CrossRef]

21. Singh, S.; Sarroza, D.; English, A.; McGrory, M.; Dong, A.; Zweifel, L.; Land, B.B.; Li, Y.; Bruchas, M.R.; Stella, N. Pharmacological Characterization of the Endocannabinoid Sensor GRAB$_{eCB2.0}$. *Cannabis Cannabinoid Res.* **2023**. [CrossRef] [PubMed]

22. Cooper, A.; Singh, S.; Hook, S.; Tyndall, J.D.A.; Vernall, A.J. Chemical Tools for Studying Lipid-Binding Class A G Protein–Coupled Receptors. *Pharmacol. Rev.* **2017**, *69*, 316–353. [CrossRef] [PubMed]

23. Ravotto, L.; Duffet, L.; Zhou, X.; Weber, B.; Patriarchi, T. A Bright and Colorful Future for G-Protein Coupled Receptor Sensors. *Front. Cell. Neurosci.* **2020**, *14*, 67. [CrossRef] [PubMed]

24. Haider, R.S.; Godbole, A.; Hoffmann, C. To sense or not to sense—New insights from GPCR-based and arrestin-based biosensors. *Curr. Opin. Cell Biol.* **2019**, *57*, 16–24. [CrossRef]

25. Zhang, R.; Xie, X. Tools for GPCR drug discovery. *Acta Pharmacol. Sin.* **2012**, *33*, 372–384. [CrossRef] [PubMed]

26. Moreira, F.A.; Grieb, M.; Lutz, B. Central side-effects of therapies based on CB1 cannabinoid receptor agonists and antagonists: Focus on anxiety and depression. *Best Pract. Res. Clin. Endocrinol. Metab.* **2009**, *23*, 133–144. [CrossRef] [PubMed]

27. Atkinson, D.L.; Abbott, J.K. Cannabinoids and the brain: The effects of endogenous and exogenous cannabinoids on brain systems and function. In *The Complex Connection between Cannabis and Schizophrenia*; Elsevier: Amsterdam, The Netherlands, 2018; pp. 37–74.

28. Milligan, A.L.; Szabo-Pardi, T.A.; Burton, M.D. Cannabinoid receptor type 1 and its role as an analgesic: An opioid alternative? *J. Dual Diagn.* **2020**, *16*, 106–119. [CrossRef] [PubMed]

29. Qureshi, J.; Saady, M.; Cardounel, A.; Kalimi, M. Identification and characterization of a novel synthetic cannabinoid CP 55,940 binder in rat brain cytosol. *Mol. Cell. Biochem.* **1998**, *181*, 21–27. [CrossRef] [PubMed]

30. Rinaldi-Carmona, M.; Pialot, F.; Congy, C.; Redon, E.; Barth, F.; Bachy, A.; Brelière, J.-C.; Soubrié, P.; Le Fur, G. Characterization and distribution of binding sites for [3H]-SR 141716A, a selective brain (CB1) cannabinoid receptor antagonist, in rodent brain. *Life Sci.* **1996**, *58*, 1239–1247. [CrossRef]

31. Darmani, N.A.; Sim-Selley, L.J.; Martin, B.R.; Janoyan, J.J.; Crim, J.L.; Parekh, B.; Breivogel, C.S. Antiemetic and motor-depressive actions of CP55,940: Cannabinoid CB1 receptor characterization, distribution, and G-protein activation. *Eur. J. Pharmacol.* **2003**, *459*, 83–95. [CrossRef]

32. Gilbert, M.T.; Sulik, K.K.; Fish, E.W.; Baker, L.K.; Dehart, D.B.; Parnell, S.E. Dose-dependent teratogenicity of the synthetic cannabinoid CP-55,940 in mice. *Neurotoxicol. Teratol.* **2016**, *58*, 15–22. [CrossRef] [PubMed]

33. Sun, J.; Fang, Y.-Q.; Ren, H.; Chen, T.; Guo, J.-J.; Yan, J.; Song, S.; Zhang, L.-Y.; Liao, H. WIN55,212-2 protects oligodendrocyte precursor cells in stroke penumbra following permanent focal cerebral ischemia in rats. *Acta Pharmacol. Sin.* **2013**, *34*, 119–128. [CrossRef] [PubMed]

34. Porcella, A.; Maxia, C.; Gessa, G.L.; Pani, L. The synthetic cannabinoid WIN55212-2 decreases the intraocular pressure in human glaucoma resistant to conventional therapies. *Eur. J. Neurosci.* **2001**, *13*, 409–412. [CrossRef] [PubMed]

35. Pérez-Diego, M.; Angelina, A.; Martín-Cruz, L.; de la Rocha-Muñoz, A.; Maldonado, A.; Sevilla-Ortega, C.; Palomares, O. Cannabinoid WIN55,212-2 reprograms monocytes and macrophages to inhibit LPS-induced inflammation. *Front. Immunol.* **2023**, *14*, 1147520. [CrossRef] [PubMed]

36. Wang, L.; Zeng, Y.; Zhou, Y.; Yu, J.; Liang, M.; Qin, L.; Zhou, Y. Win55,212-2 improves neural injury induced by HIV-1 glycoprotein 120 in rats by exciting CB$_2$R. *Brain Res. Bull.* **2022**, *182*, 67–79. [CrossRef] [PubMed]

37. Herzberg, U.; Eliav, E.; Bennett, G.; Kopin, I.J. The analgesic effects of R(+)-WIN 55,212–2 mesylate, a high affinity cannabinoid agonist, in a rat model of neuropathic pain. *Neurosci. Lett.* **1997**, *221*, 157–160. [CrossRef] [PubMed]

38. An, D.; Peigneur, S.; Hendrickx, L.A.; Tytgat, J. Targeting Cannabinoid Receptors: Current Status and Prospects of Natural Products. *Int. J. Mol. Sci.* **2020**, *21*, 5064. [CrossRef] [PubMed]

39. Li, X.; Hua, T.; Vemuri, K.; Ho, J.H.; Wu, Y.; Wu, L.; Popov, P.; Benchama, O.; Zvonok, N.; Qu, L.; et al. Crystal structure of the human cannabinoid receptor CB2. *Cell* **2019**, *176*, 459–467.e13. [CrossRef] [PubMed]

40. Nguyen, T.; Thomas, B.F.; Zhang, Y. Overcoming the Psychiatric Side Effects of the Cannabinoid CB1 Receptor Antagonists: Current Approaches for Therapeutics Development. *Curr. Top. Med. Chem.* **2019**, *19*, 1418–1435. [CrossRef]

41. Shao, Z.; Yin, J.; Chapman, K.; Grzemska, M.; Clark, L.; Wang, J.; Rosenbaum, D.M. High-resolution crystal structure of the human CB1 cannabinoid receptor. *Nature* **2016**, *540*, 602–606. [CrossRef]

42. Patel, P.N.; Pathak, R. Rimonabant: A novel selective cannabinoid-1 receptor antagonist for treatment of obesity. *Am. J. Health Pharm.* **2007**, *64*, 481–489. [CrossRef] [PubMed]

43. Iyer, M.R.; Cinar, R.; Liu, J.; Godlewski, G.; Szanda, G.; Puhl, H.; Ikeda, S.R.; Deschamps, J.; Lee, Y.-S.; Steinbach, P.J.; et al. Structural Basis of Species-Dependent Differential Affinity of 6-Alkoxy-5-Aryl-3-Pyridinecarboxamide Cannabinoid-1 Receptor Antagonists. *Mol. Pharmacol.* **2015**, *88*, 238–244. [CrossRef] [PubMed]

44. Ramesh, K.; Rosenbaum, D.M. Molecular basis for ligand modulation of the cannabinoid CB_1 receptor. *Br. J. Pharmacol.* **2022**, *179*, 3487–3495. [CrossRef] [PubMed]

45. Wagner, J.D.; Zhang, L.; Kavanagh, K.; Ward, G.M.; Chin, J.E.; Hadcock, J.R.; Auerbach, B.J.; Harwood, H.J. A Selective Cannabinoid-1 Receptor Antagonist, PF-95453, Reduces Body Weight and Body Fat to a Greater Extent than Pair-Fed Controls in Obese Monkeys. *J. Pharmacol. Exp. Ther.* **2010**, *335*, 103–113. [CrossRef] [PubMed]

46. Griffith, D.A.; Hadcock, J.R.; Black, S.C.; Iredale, P.A.; Carpino, P.A.; DaSilva-Jardine, P.; Day, R.; DiBrino, J.; Dow, R.L.; Landis, M.S.; et al. Discovery of 1-[9-(4-chlorophenyl)-8-(2-chlorophenyl)-9H-purin-6-yl]-4-ethylaminopiperidine-4-carboxylic acid amide hydrochloride (CP-945,598), a novel, potent, and selective cannabinoid type 1 receptor antagonist. *J. Med. Chem.* **2009**, *52*, 234–237. [CrossRef] [PubMed]

47. Chorvat, R.J. Peripherally restricted CB1 receptor blockers. *Bioorg. Med. Chem. Lett.* **2013**, *23*, 4751–4760. [CrossRef] [PubMed]

48. Iyer, M.R.; Cinar, R.; Coffey, N.J.; Kunos, G. Synthesis of 13 C6-labeled, dual-target inhibitor of cannabinoid-1 receptor (CB1 R) and inducible nitric oxide synthase (iNOS). *J. Labelled Comp. Radiopharm.* **2018**, *61*, 773–779. [CrossRef] [PubMed]

49. Liu, Z.; Iyer, M.R.; Godlewski, G.; Jourdan, T.; Liu, J.; Coffey, N.J.; Zawatsky, C.N.; Puhl, H.L.; Wess, J.; Meister, J.; et al. Functional Selectivity of a Biased Cannabinoid-1 Receptor (CB_1R) Antagonist. *ACS Pharmacol. Transl. Sci.* **2021**, *4*, 1175–1187. [CrossRef] [PubMed]

50. Cinar, R.; Iyer, M.R.; Liu, Z.; Cao, Z.; Jourdan, T.; Erdelyi, K.; Godlewski, G.; Szanda, G.; Liu, J.; Park, J.K.; et al. Hybrid inhibitor of peripheral cannabinoid-1 receptors and inducible nitric oxide synthase mitigates liver fibrosis. *J. Clin. Investig.* **2016**, *1*, e87336. [CrossRef]

51. Iyer, M.R.; Cinar, R.; Katz, A.; Gao, M.; Erdelyi, K.; Jourdan, T.; Coffey, N.J.; Pacher, P.; Kunos, G. Design, Synthesis, and Biological Evaluation of Novel, Non-Brain-Penetrant, Hybrid Cannabinoid CB1R Inverse Agonist/Inducible Nitric Oxide Synthase (iNOS) Inhibitors for the Treatment of Liver Fibrosis. *J. Med. Chem.* **2017**, *60*, 1126–1141. [CrossRef]

52. Iyer, M.R.; Cinar, R.; Wood, C.M.; Zawatsky, C.N.; Coffey, N.J.; Kim, K.A.; Liu, Z.; Katz, A.; Abdalla, J.; Hassan, S.A.; et al. Synthesis, Biological Evaluation, and Molecular Modeling Studies of 3,4-Diarylpyrazoline Series of Compounds as Potent, Nonbrain Penetrant Antagonists of Cannabinoid-1 (CB1R) Receptor with Reduced Lipophilicity. *J. Med. Chem.* **2022**, *65*, 2374–2387. [CrossRef] [PubMed]

53. Dvorácskó, S.; Herrerias, A.; Oliverio, A.; Bhattacharjee, P.; Pommerolle, L.; Liu, Z.; Feng, D.; Lee, Y.-S.; Hassan, S.A.; Godlewski, G.; et al. Cannabinoformins: Designing Biguanide-Embedded, Orally Available, Peripherally Selective Cannabinoid-1 Receptor Antagonists for Metabolic Syndrome Disorders. *J. Med. Chem.* **2023**, *66*, 11985–12004. [CrossRef] [PubMed]

54. Santos-Molina, L.; Herrerias, A.; Zawatsky, C.N.; Gunduz-Cinar, O.; Cinar, R.; Iyer, M.R.; Wood, C.M.; Lin, Y.; Gao, B.; Kunos, G.; et al. Effects of a Peripherally Restricted Hybrid Inhibitor of CB1 Receptors and iNOS on Alcohol Drinking Behavior and Alcohol-Induced Endotoxemia. *Molecules* **2021**, *26*, 5089. [CrossRef] [PubMed]

55. Roger, C.; Buch, C.; Muller, T.; Leemput, J.; Demizieux, L.; Passilly-Degrace, P.; Cinar, R.; Iyer, M.R.; Kunos, G.; Vergès, B.; et al. Simultaneous Inhibition of Peripheral CB1R and iNOS Mitigates Obesity-Related Dyslipidemia Through Distinct Mechanisms. *Diabetes* **2020**, *69*, 2120–2132. [CrossRef] [PubMed]

56. Zawatsky, C.N.; Park, J.K.; Abdalla, J.; Kunos, G.; Iyer, M.R.; Cinar, R. Peripheral Hybrid CB1R and iNOS Antagonist MRI-1867 Displays Anti-Fibrotic Efficacy in Bleomycin-Induced Skin Fibrosis. *Front. Endocrinol.* **2021**, *12*, 744857. [CrossRef]

57. Cinar, R.; Park, J.K.; Zawatsky, C.N.; Coffey, N.J.; Bodine, S.P.; Abdalla, J.; Yokoyama, T.; Jourdan, T.; Jay, L.; Zuo, M.X.G.; et al. CB_1R and iNOS are distinct players promoting pulmonary fibrosis in Hermansky–Pudlak syndrome. *Clin. Transl. Med.* **2021**, *11*, e471. [CrossRef]

58. Crater, G.D.; Lalonde, K.; Ravenelle, F.; Harvey, M.; Després, J.-P. Effects of CB1R inverse agonist, INV-202, in patients with features of metabolic syndrome. A randomized, placebo-controlled, double-blind phase 1b study. *Diabetes Obes. Metab.* **2023**, *26*, 642–649. [CrossRef] [PubMed]

59. Chorvat, R.J.; Berbaum, J.; Seriacki, K.; McElroy, J.F. JD-5006 and JD-5037: Peripherally restricted (PR) cannabinoid-1 receptor blockers related to SLV-319 (Ibipinabant) as metabolic disorder therapeutics devoid of CNS liabilities. *Bioorg. Med. Chem. Lett.* **2012**, *22*, 6173–6180. [CrossRef]

60. Lange, J.H.; Coolen, H.K.; van Stuivenberg, H.H.; Dijksman, J.A.; Herremans, A.H.; Ronken, E.; Keizer, H.G.; Tipker, K.; McCreary, A.C.; Veerman, W.; et al. Synthesis, biological properties, and molecular modeling investigations of novel 3,4-diarylpyrazolines as potent and selective CB(1) cannabinoid receptor antagonists. *J. Med. Chem.* **2004**, *47*, 627–643. [CrossRef]

61. Janero, D.R.; Thakur, G.A. Leveraging allostery to improve G protein-coupled receptor (GPCR)-directed therapeutics: Cannabinoid receptor 1 as discovery target. *Expert Opin. Drug Discov.* **2016**, *11*, 1223–1237. [CrossRef]

62. Ross, R.A. Allosterism and cannabinoid CB1 receptors: The shape of things to come. *Trends Pharmacol. Sci.* **2007**, *28*, 567–572. [CrossRef] [PubMed]

63. Klein, M.T.; Vinson, P.N.; Niswender, C.M. Approaches for probing allosteric interactions at 7 transmembrane spanning receptors. *Prog. Mol. Biol. Transl. Sci.* **2013**, *115*, 1–59. [PubMed]

64. Morales, P.; Goya, P.; Jagerovic, N.; Hernandez-Folgado, L. Allosteric Modulators of the CB_1 Cannabinoid Receptor: A Structural Update Review. *Cannabis Cannabinoid Res.* **2016**, *1*, 22–30. [CrossRef] [PubMed]

65. Dopart, R.; Lu, D.; Lichtman, A.H.; Kendall, D.A. Allosteric modulators of cannabinoid receptor 1: Developing compounds for improved specificity. *Drug Metab. Rev.* **2018**, *50*, 3–13. [CrossRef] [PubMed]

66. Price, M.R.; Baillie, G.L.; Thomas, A.; Stevenson, L.A.; Easson, M.; Goodwin, R.; McLean, A.; McIntosh, L.; Goodwin, G.; Walker, G.; et al. Allosteric Modulation of the Cannabinoid CB_1 Receptor. *Mol. Pharmacol.* **2005**, *68*, 1484–1495. [CrossRef] [PubMed]

67. Ahn, K.H.; Mahmoud, M.M.; Kendall, D.A. Allosteric Modulator ORG27569 Induces CB1 Cannabinoid Receptor High Affinity Agonist Binding State, Receptor Internalization, and Gi Protein-independent ERK1/2 Kinase Activation. *J. Biol. Chem.* **2012**, *287*, 12070–12082. [CrossRef]

68. Horswill, J.G.; Bali, U.; Shaaban, S.; Keily, J.F.; Jeevaratnam, P.; Babbs, A.J.; Reynet, C.; Wong Kai In, P. PSNCBAM-1, a novel allosteric antagonist at cannabinoid CB1 receptors with hypophagic effects in rats. *Br. J. Pharmacol.* **2007**, *152*, 805–814. [CrossRef] [PubMed]

69. Arunlakshana, O.; Schild, H.O. Some quantitative uses of drug antagonists. *Br. J. Pharmacol. Chemother.* **1959**, *14*, 48–58. [CrossRef]

70. Laprairie, R.B.; Kulkarni, P.M.; Deschamps, J.R.; Kelly, M.E.M.; Janero, D.R.; Cascio, M.G.; Stevenson, L.A.; Pertwee, R.G.; Kenakin, T.P.; Denovan-Wright, E.M.; et al. Enantiospecific Allosteric Modulation of Cannabinoid 1 Receptor. *ACS Chem. Neurosci.* **2017**, *8*, 1188–1203. [CrossRef]

71. Thomas, M.; Lu, B.; Breschi, J.J.; Ge, Q.; Zhang, C.; Chen, J.; Klibanov, A.M. Fulldeacylation of polyethylenimine dramatically boosts itsgene delivery efficiency and specificity to mouse lung. *Proc. Natl. Acad. Sci. USA* **2005**, *102*, 5679–5684.

72. Calderone, V.; Baragatti, B.; Breschi, M.; Martinotti, E. Experimental and theoretical comparisons between the classical Schild analysis and a new alternative method to evaluate the pA2 of competitive antagonists. *Naunyn-Schmiedeberg's Arch. Pharmacol.* **1999**, *360*, 477–487. [CrossRef]

73. Lew, M.; Angus, J. Analysis of competitive agonist-antagonist interactions by nonlinear regression. *Trends Pharmacol. Sci.* **1995**, *16*, 328–337. [CrossRef] [PubMed]

74. Lin, L.S.; Lanza, T.J.; Jewell, J.P.; Liu, P.; Shah, S.K.; Qi, H.; Tong, X.; Wang, J.; Xu, S.S.; Fong, T.M.; et al. Discovery of N-[(1S,2S)-3-(4-Chlorophenyl)-2- (3-Cyanophenyl)-1-Methylpropyl]-2-Methyl- {[5-(Trifluoromethyl)Pyridin-2-Yl]Oxy}propanamide (MK-0364), a Novel, Acyclic Cannabinoid-1 Receptor Inverse Agonist for the Treatment of Obesity. *J. Med. Chem.* **2006**, *49*, 7584–7587. [CrossRef] [PubMed]